LETTER

doi:10.1038/nature16137

Collisionless encounters and the origin of the lunar inclination

Kaveh Pahlevan[1] & Alessandro Morbidelli[1]

The Moon is generally thought to have formed from the debris ejected by the impact of a planet-sized object with the proto-Earth towards the end of planetary accretion[1,2]. Models of the impact process predict that the lunar material was disaggregated into a circumplanetary disk and that lunar accretion subsequently placed the Moon in a near-equatorial orbit[3–6]. Forward integration of the lunar orbit from this initial state predicts a modern inclination at least an order of magnitude smaller than the lunar value—a long-standing discrepancy known as the lunar inclination problem[7–9]. Here we show that the modern lunar orbit provides a sensitive record of gravitational interactions with Earth-crossing planetesimals that were not yet accreted at the time of the Moon-forming event. The currently observed lunar orbit can naturally be reproduced via interaction with a small quantity of mass (corresponding to 0.0075–0.015 Earth masses eventually accreted to the Earth) carried by a few bodies, consistent with the constraints and models of late accretion[10,11]. Although the encounter process has a stochastic element, the observed value of the lunar inclination is among the most likely outcomes for a wide range of parameters. The excitation of the lunar orbit is most readily reproduced via collisionless encounters of planetesimals with the Earth–Moon system with strong dissipation of tidal energy on the early Earth. This mechanism obviates the need for previously proposed (but idealized) excitation mechanisms[12,13], places the Moon-forming event in the context of the formation of Earth, and constrains the pristineness of the dynamical state of the Earth–Moon system.

The Moon-forming impact is thought to have generated a compact circumplanetary disk (within ten Earth radii, R_E) of debris out of which the Moon rapidly accreted. Like Saturn's rings, the proto-lunar disk would be expected to become equatorial on a timescale that is rapid relative to its evolutionary timescale. Hence, so long as the proto-lunar material disaggregated into a disk following the giant impact, the Moon is expected to have accreted within about one degree of the Earth's equatorial plane[6]. Tidal evolution calculations suggest that for every degree of inclination of the lunar orbital plane relative to the Earth's equatorial plane at an Earth–Moon separation of $10R_E$, the current lunar orbit would exhibit about half a degree of inclination relative to Earth's orbital plane[7–9]. The modern lunar inclination of approximately 5° would—without external influences—translate to an inclination of about 10° to Earth's equatorial plane at $10R_E$ shortly after lunar accretion. This approximately tenfold difference between theoretical expectations of lunar accretion and the observed Earth–Moon system is known as the lunar inclination problem.

Previous work on this problem has sought to identify mechanisms such as a gravitational resonance between the newly formed Moon and the Sun[12] or the remnant proto-lunar disk[13] that can excite the lunar inclination to a level consistent with its current value. Neither of these scenarios is satisfactory, however, as the former requires particular values of the tidal dissipation parameters and the latter has only been shown to be viable in an idealized system in which a single, fully formed Moon interacts with a single pair of resonances in the proto-lunar disk. Moreover, previous works assumed that the excitation of the lunar orbit was determined during interactions that essentially coincided with lunar origin. Here, we propose that the lunar inclination arose much later as a consequence of the sweep-up of remnant planetesimals in the inner Solar System.

After the giant impact and at most 10^3 years[14,15], the Moon has accreted, interacted with[13] and caused the collapse of the remnant proto-lunar disk onto the Earth[6], passed the evection resonance with the Sun[3,12,16], and begun a steady outward tidal evolution. On a timescale (10^6–10^7 years) that is rapid relative to that characterizing depletion of planetesimals in the final post-Moon-formation stage of planetary accretion[17] (called 'late accretion'), the lunar orbit expands, owing to the action of tides, to an Earth–Moon separation of $20R_E$–$40R_E$. During this time, the lunar orbit transitions from precession around the spin axis of Earth to precession around the normal vector of the heliocentric orbit[8], and its inclination becomes insensitive to the shifting of the Earth's equatorial plane via subsequent accretion[18]. However, as we show, lunar inclination becomes more sensitive to gravitational interactions with passing planetesimals as the tidal evolution of the system proceeds. The sensitivity is such that it renders the lunar orbital excitation a natural outcome of the sweep-up of the leftovers of accretion and yields a new constraint on the dynamical and tidal environment of the Earth–Moon system in the 10^8 years immediately following its origin.

Although subsequent collisions with the Earth–Moon system have been previously considered as a mechanism for dynamical excitation[18], the collision of inner Solar System bodies with the Earth tends to be preceded by a large number (10^3–10^4) of collisionless encounters. Excitation via this process is governed by two relevant timescales: the timescale over which remnant populations in the inner Solar System are lost via accretion onto the planets and the Sun (several tens of millions of years[17]); and the timescale for the lunar tidal orbital expansion, which is a rapidly varying function of the Earth–Moon distance. The Earth–Moon distance is important because it determines the system cross-section for collisionless encounters with remnant bodies. Accordingly, the rate of tidal expansion of the lunar orbit during the first approximately 10^8 years after the giant impact is also important. As tidal evolution proceeds and the Earth–Moon separation increases, the system becomes increasingly susceptible to collisionless excitation, while populations capable of exciting the system are progressively depleted. A few tens of millions of years after the Moon-forming event, the Earth–Moon system reaches an optimal capacity for excitation via gravitational encounters: a dynamically excitable system co-existing with a substantial remnant-body population.

Here, we run a series of Monte Carlo simulations to set constraints on the outcome of repeated encounters of massive bodies with the evolving Earth–Moon system. The simulations are carried out until the populations are exhausted either through collision with the Earth or through non-terrestrial loss channels (for details, see Methods). A sample run of dynamical excitation during the first approximately 10^8 years of Earth–Moon history is shown in Fig. 1. No single event dominates: several strong encounters contribute substantially to the

[1]Laboratoire Lagrange, Université Côte d'Azur, Observatoire de la Côte d'Azur, CNRS Boulevard de l'Observatoire CS 34229, 06304 Nice Cedex 4, France.

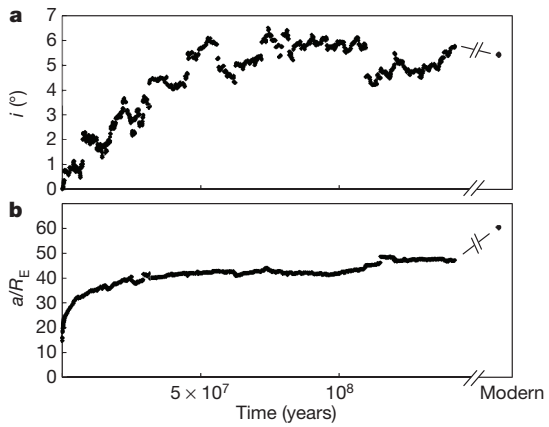

Figure 1 | Sample realization. a, **b**, A model of the early lunar orbit subject to tidal evolution ($k_2/Q = 0.1$) and encounters leading to collision of two $0.00375M_E$ bodies with the Earth. The semi-major axis of the evolving lunar orbit a is given in Earth radii (shown in **b**). Although not every encounter increases the lunar inclination i, the cumulative effect shows a tendency towards excitation (shown in **a**). Notable interactions include merging collisions with the Earth kicking the lunar orbit via recoil (at 29.1 Myr and 31.5 Myr), several exceptionally close encounters with the Moon (at 7.3 Myr and 109.6 Myr) and the exhaustion of the population (at 141.7 Myr) ultimately marking the end of the simulation. Subsequent inclination damping owing to planetary tides is modest (from 5.8° at $47R_E$ at the end of the simulation to 5.4° at $60R_E$), a feature that is typical of this 'late' excitation mechanism.

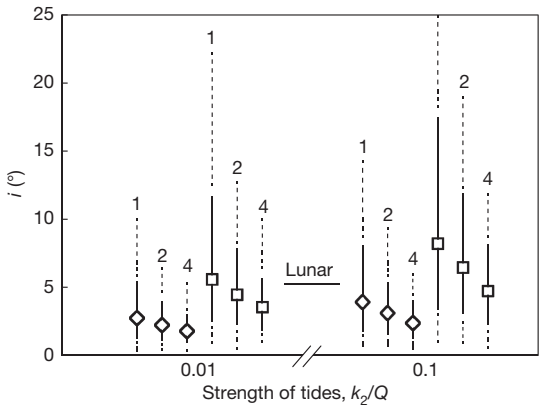

Figure 2 | Summary of simulations. Median values (symbols), and 1σ (solid lines) and 2σ (dashed lines) intervals for the lunar inclination i at the end of the simulations after damping via planetary tides to the modern Earth–Moon separation. The excitation in the modern lunar orbit is plotted for comparison, indicated by the horizontal line labelled 'lunar'. Diamonds correspond to simulations with $0.0075M_E$ accreted to Earth; squares correspond to $0.015M_E$. 'Strong' tidal dissipation ($k_2/Q = 0.1$) corresponds to a hot dissipative silicate Earth, and 'weak' dissipation ($k_2/Q = 0.01$) represents the geologic average value dominated by dissipation in shallow oceans. In these simulations, the accretion of $0.0075M_E$ (with 'strong' tides) to $0.015M_E$ (with 'weak' tides) frequently reproduces the excitation in the lunar orbit. The number of bodies delivering the late accreted mass in each set of simulations is reported above each symbol.

final excitation. The size distribution of the late-accreting population is assumed to be top heavy, with most of the mass contained in a few massive bodies, as has been previously proposed to explain terrestrial late accretion[10,11]. This particular simulation ultimately results in two $0.00375M_E$ planetesimals (where M_E is Earth's mass) left over from the formation process colliding with the Earth. Tidal damping of the lunar inclination is applied along with the lunar orbital expansion, following equation (1) (see Methods). We do not consider the possibility that the lunar inclination might have been more strongly damped via dissipation in the lunar magma ocean, as recently proposed[19]. In the Methods, we show that this effect is not important as long as the lunar magma ocean crystallized within a few tens of millions of years.

Lunar orbital excitation in this epoch depends on the total mass of leftover planetesimals, the number of bodies carrying the mass and their orbital distribution, the rate of terrestrial tidal dissipation, and a stochastic element. In Fig. 2, we show results of simulations of the excitation of the lunar inclination due to interaction of the system with a small amount of mass (equivalent to $0.0075M_E$–$0.015M_E$ eventually accreted to the Earth), for different values of the strength of tidal dissipation and the number of bodies delivering the mass (which is constrained to be <20 colliding with Earth via models of late accretion[10,11]).

Several features are apparent. First, there is a quasi-linear dependence of the excitation on the total mass of late accretion: other variables being equal, excitation corresponding to $0.015M_E$ of late accretion is approximately twice as great as that with $0.0075M_E$. The mass accreted onto the Earth thereby provides a proxy for collisionless excitation. Second, the lunar orbital excitation exhibits some dependence on the strength of tidal evolution: stronger dissipation within the Earth drives the lunar orbit outwards faster and exposes the system to more collisionless events. Simulations with the weakest tides that we considered—characterized by the ratio of the tidal Love number to the specific dissipation function $k_2/Q = 0.01$—typically excite the lunar inclination with a planetesimal population consistent with $0.015M_E$ of late accretion, whereas with stronger tidal dissipation ($k_2/Q = 0.1$), lunar inclination is routinely excited by a planetesimal population carrying $0.0075M_E$ of late accretion. Third, there exists a negative dependence of the excitation on the number of bodies involved in late accretion, such that the mechanism requires a population that is top heavy (with most of the mass delivered via the most massive bodies). For a given mass of late accretion, a greater number of bodies also renders the distribution of lunar inclinations more strongly peaked and predictions of the expected excitation more precise. Despite an order of magnitude of uncertainty in the strength of early terrestrial tides (k_2/Q) and in the number of bodies involved in the leftover population, and the stochasticity that is inherent in collisionless encounters, close encounters with a population of planetesimals delivering $0.0075M_E$–$0.015M_E$ to the Earth after the Moon-forming event can robustly reproduce the excitation that characterizes the lunar orbit.

The angular momentum of the Earth–Moon system at the time of its origin is a central feature diagnostic of various proposed giant-impact scenarios[1,3,4,18]. Given that the lunar orbit provides a sensitive dynamical measure of encounters with the Earth after the origin of the Moon, we ask whether such gravitational interactions were effective in injecting or extracting angular momentum. Figure 3 summarizes the angular momentum change versus the final excitation. The change in angular momentum corresponding to the modern inclination excitation of approximately 5° is probably a few tens per cent or less. Hence, the standard giant-impact scenario[4] followed by little subsequent dynamical modification is compatible with the dynamical state of the modern system, whereas a high-angular-momentum impact scenario[3,5] would require another dynamical mechanism such as the evection resonance[3,12,16] to be reconciled with the modern Earth–Moon system.

The sensitivity of the orbits of impact-generated satellites to ongoing accretion onto the host planet has several consequences. The degree of orbital excitation resulting from interaction with, and accretion of, $0.0075M_E$–$0.015M_E$ onto the early Earth suggests that collisionless encounters with massive bodies—such as the Moon-to-Mars mass embryos thought to have played a key role in the accretion of the Earth—would have excited satellites to very eccentric orbits ultimately leading to their dynamical loss, either via collision with the host planet or liberation into heliocentric orbit. Such excitability of impact-generated satellite orbits may explain several features of the inner Solar System that have yet to be understood. For example, despite impact-generated satellites being a quasi-generic feature of terrestrial planet formation via giant impact, the absence of an impact-generated

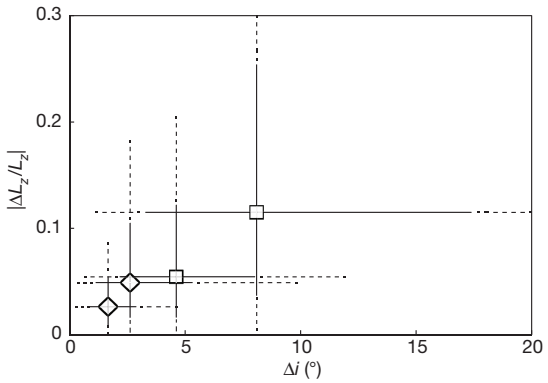

Figure 3 | Angular momentum change of the Earth–Moon system. Median values (symbols), and 1σ (solid lines) and 2σ (dashed lines) intervals for inclination i and angular momentum L_z change via post-lunar collisionless encounters. Diamonds represent realizations with weak tides ($k_2/Q = 0.01$) and $0.0075M_E$ accretion; squares correspond to realizations with stronger dissipation ($k_2/Q = 0.1$) and $0.015M_E$ accretion, bracketing the range in our simulations. Each suite of simulations is composed of two subsets: one with late accretion delivered via one body (greater excitation); the other, four bodies (lesser excitation). Intermediate outcomes with two accreted bodies are omitted for clarity. For a level of excitation consistent with the modern lunar orbit (5.15°), the amount of system angular momentum change is probably $<20\%$. However, the 2σ intervals for the strongest excitation case plotted extend to $\Delta i = 42°$ and $|\Delta L_z/L_z| = 0.48$, implying a small probability ($<5\%$) for angular momentum change $>50\%$.

satellite around Venus[20] and the apparent absence of a pre-Moon terrestrial satellite[21] can be understood: any such early-formed satellites would have been lost via encounters with extant planetary embryos, including perhaps the Moon-forming impactor itself. Moreover, the occurrence of the Moon-forming giant impact late in the history of Earth accretion can be understood as a necessity for its survival: even satellites generated moderately earlier would have been readily dynamically destabilized. Just as the survival of planets depends on the surrounding stellar environment[22], the survival of an impact-generated satellite depends on the planetary environment at the time of origin.

Online Content Methods, along with any additional Extended Data display items and Source Data, are available in the online version of the paper; references unique to these sections appear only in the online paper.

Received 23 March; accepted 6 October 2015.

1. Cameron, A. G. W. & Ward, W. R. The origin of the Moon. *Lunar Planet. Sci. Conf.* **7,** abstr. 120–122 (1976).
2. Hartmann, W. K. & Davis, D. R. Satellite-sized planetesimals and lunar origin. *Icarus* **24,** 504–515 (1975).
3. Cuk, M. & Stewart, S. T. Making the Moon from a fast-spinning Earth: a giant impact followed by resonant despinning. *Science* **338,** 1047–1052 (2012).
4. Canup, R. M. & Asphaug, E. Origin of the Moon in a giant impact near the end of the Earth's formation. *Nature* **412,** 708–712 (2001).
5. Canup, R. M. Forming a Moon with an Earth-like composition via a giant impact. *Science* **338,** 1052–1055 (2012).
6. Ida, S., Canup, R. M. & Stewart, G. R. Lunar accretion from an impact-generated disk. *Nature* **389,** 353–357 (1997).
7. Mignard, F. The lunar orbit revisited, III. *Moon Planets* **24,** 189–207 (1981).
8. Goldreich, P. History of lunar orbit. *Rev. Geophys.* **4,** 411–439 (1966).
9. Touma, J. & Wisdom, J. Evolution of the Earth–Moon system. *Astron. J.* **108,** 1943–1961 (1994).
10. Bottke, W. F., Walker, R. J., Day, J. M. D., Nesvorny, D. & Elkins-Tanton, L. Stochastic late accretion to Earth, the Moon, and Mars. *Science* **330,** 1527–1530 (2010).
11. Raymond, S. N., Schlichting, H. E., Hersant, F. & Selsis, F. Dynamical and collisional constraints on a stochastic late veneer on the terrestrial planets. *Icarus* **226,** 671–681 (2013).
12. Touma, J. & Wisdom, J. Resonances in the early evolution of the Earth-Moon system. *Astron. J.* **115,** 1653–1663 (1998).
13. Ward, W. R. & Canup, R. M. Origin of the Moon's orbital inclination from resonant disk interactions. *Nature* **403,** 741–743 (2000).
14. Thompson, C. & Stevenson, D. J. Gravitational instability in two-phase disks and the origin of the Moon. *Astrophys. J.* **333,** 452–481 (1988).
15. Salmon, J. & Canup, R. M. Lunar accretion from a Roche-interior fluid disk. *Astrophys. J.* **760,** 83 (2012).
16. Wisdom, J. & Tian, Z. L. Early evolution of the Earth–Moon system with a fast-spinning Earth. *Icarus* **256,** 138–146 (2015).
17. Morbidelli, A., Marchi, S., Bottke, W. F. & Kring, D. A. A sawtooth-like timeline for the first billion years of lunar bombardment. *Earth Planet. Sci. Lett.* **355–356,** 144–151 (2012).
18. Canup, R. M. Dynamics of lunar formation. *Annu. Rev. Astron. Astrophys.* **42,** 441–475 (2004).
19. Nimmo, F. & Chen, E. M. A. Tidal dissipation in the early lunar magma ocean and its role in the evolution of the Earth-Moon system. *45th Lunar Planet. Sci. Conf.* abstr. 1459 (2014).
20. Alemi, A. & Stevenson, D. J. Why Venus has no moon. *Bull. Am. Astron. Soc.* **38,** 491 (2006).
21. Canup, R. M. Lunar-forming impacts: processes and alternatives. *Philos. Trans. R. Soc. London Ser. A* **372,** 20130175 (2014).
22. Spurzem, R., Giersz, M., Heggie, D. C. & Lin, D. N. C. Dynamics of planetary systems in star clusters. *Astrophys. J.* **697,** 458–482 (2009).

Acknowledgements This research was carried out as part of a Henri Poincaré Fellowship at the Observatoire de la Côte d'Azur (OCA) to K.P. The Henri Poincaré Fellowship is funded by the OCA and the City of Nice, France. A.M. thanks the European Research Council Advanced Grant ACCRETE (no. 290568).

Author Contributions K.P. and A.M. discussed every step of the project, designed the simulation set-up and co-wrote the numerical code. K.P. performed the simulations and the statistical analysis.

Author Information Reprints and permissions information is available at www.nature.com/reprints. The authors declare no competing financial interests. Readers are welcome to comment on the online version of the paper. Correspondence and requests for materials should be addressed to K.P. (pahlevan@oca.eu).

METHODS

A large number of simulations (about 10^3) are required to characterize the distribution of outcomes for repeated encounters of a given planetesimal population with a given early Earth–Moon system. Accordingly, we design a numerical experiment that captures the physics of the problem statistically and that can be computed efficiently. Heliocentric orbits for late-accreting planetesimal populations were generated according to a Rayleigh distribution with a Rayleigh eccentricity $e_R = 0.3$ and inclination $i_R = e_R/2$; these values are consistent with simulations of terrestrial planet formation[23]. To test for sensitivity to population orbits, we varied e_R between 0.3 and 0.4; the resulting median inclination excitation changed by less than 10%. With given orbital distributions, the subset of the population that is Earth-crossing was selected and encounter probabilities with the Hill radius (R_H) of the Earth were calculated according to expressions given in ref. 24. The masses of the planetesimals are assumed to be in the range $0.15M_L$–$1.2M_L$ (M_L is the lunar mass), consistent with those expected for the projectiles carrying the Earth's late accretion[10]. At the beginning of the simulations, the Earth and the Moon were placed on circular uninclined orbits with radii of 1 AU and $5R_E$, respectively, near their orbits at the end of accretion and the beginning of tidal history. An encounter time and encounter orbit were chosen randomly according to the distribution of Earth-crossing planetesimal encounter probabilities. At the time of each encounter, phases for the lunar orbit, characterized by the argument of perigee (ω), the longitude of the ascending node (Ω) and the mean anomaly (M) were selected randomly, as was the orientation of the planetesimal orbit, within those orientations admitted by the selected orbital parameters. The impact parameter (b) was selected in the interval $[0, R_H]$ according to a uniform encounter probability per unit area ($dP \propto b\,db$). Gravitational three-body (Earth–Moon–planetesimal) encounters were integrated with a Bulirsch–Stoer integrator (included in the SWIFT package) in a geocentric reference frame, tracking changes to the lunar orbit. In between three-body encounters, the eccentricity (e) and semi-major axis (a) of the lunar orbit were evolved with a constant-Q tidal model[25] while the lunar inclination was evolved with a model[26] for planetary tides:

$$\frac{di}{i} = -\frac{1}{4}\frac{da}{a} \quad (1)$$

Impacts with the Earth were assumed to be inelastic merging events with the final body carrying the total mass and momentum. Impacts onto the Moon would have been in the erosive and/or catastrophic disruption regime and realizations with such events were removed from the subsequent analysis (discussed below).

Remnant planetesimals can, in general, be eliminated via collision with the terrestrial planets and the Sun or dynamical ejection from the inner Solar System[11]. We characterize such losses using the outcome of direct N-body simulations that trace the evolution of such early planetesimals, yielding a tenfold depletion of the Earth-crossing population in the first 100 Myr, which corresponds to a population decay law of approximately $\exp(-t/\tau_{SS})$, where t is time and τ_{SS} is the time constant for the decay of the population (approximately 44 Myr) (ref. 17). Although the modern near-Earth-object population is resupplied by the asteroid belt in a quasi-steady state fashion and effectively does not decay, the leftover planetesimal population is not resupplied by a larger reservoir and therefore does decay. Owing to partial resupply of Earth-crossing bodies, the timescale for the decay of the Earth-crossing population can nevertheless be different to the lifetime of individual particles. To integrate the decay rates of Earth-crossing planetesimals using our simulations, we use the following procedure. After generating orbital populations, but before running three-body integrations, we allow the Earth-crossing populations to encounter the Earth alone, which permits derivation of a time constant for decay of this population solely via collision with the Earth ($\tau_E = 79$ Myr). Next, we require that the Earth-crossing planetesimal population in our three-body simulations decay at the same average rate as that observed in the N-body heliocentric simulations. We therefore decompose average loss rates of the Earth-crossing population into terrestrial and non-terrestrial loss modes ($1/\tau_{SS} = 1/\tau_E + 1/\tau_{NE}$), and thereby derive a time constant ($\tau_{NE} = 99$ Myr) for removal via non-terrestrial loss channels. Accordingly, we stochastically remove bodies from the population in our three-body simulations such that the average loss rate of Earth-crossing planetesimals—through collision with Earth (explicit) as well as through other modes of loss (implicit)—is consistent with the average loss rates observed in N-body simulations of late accretion[17] (see Extended Data Fig. 1a).

Each data point in Fig. 2 is the result of 4,000 realizations. To analyse the results, certain realizations were eliminated. These realizations fall into three categories: those that result in (1) a collision of a planetesimal with the Moon; (2) dynamical loss of the Moon; and (3) too large or too small a mass accreted by the Earth.

(1) Occasionally, one of the planetesimals in our simulations collides with the Moon rather than with the Earth. For simulations that deliver the late-accreted mass to Earth via one, two and four planetesimals, the fraction of realizations in which such an event takes place is 9%, 15% and 25%, respectively. Given the masses that we assume for the planetesimals ($0.15M_L$–$1.2M_L$), it is doubtful that the Moon ever experienced such a massive collision. The largest lunar impact for which we have clear and unambiguous evidence is the South Pole Aitken Basin event (an approximately 10^{34} erg event[27]), which, at the encounter velocities considered here (see Extended Data Fig. 1b), corresponds to a lunar impactor that is 3–4 orders of magnitude less massive than the planetesimals in our populations. Although most basin-forming impacts are thought to have occurred during the late accretion era[17], the effect of these impacts on the lunar inclination was minor[18].

(2) Certain realizations, particularly those that correspond with the strongest tides and largest amount of interacting mass, generate excitations in eccentricity that are sufficient to destabilize the satellite orbit. Hence, collision with the host planet or (more rarely) liberation of the satellite into heliocentric orbit follows.

(3) The total amount of planetesimal mass at the start of simulations was chosen such that, on average, the mass accreted by the Earth would be $0.0075M_E$ or $0.015M_E$, hereafter denoted the 'target mass'. Given the stochasticity inherent to this problem, the accreted mass varies between realizations, resulting in a distribution of outcomes centred on the target mass. To facilitate the expression of the results in terms of late-accreted mass, we eliminate from the subsequent analysis those realizations whose accreted mass is greater than or less than the target mass.

Differential momentum transfer is the process underlying this excitation mechanism. For simplicity, we describe this process for the case of a planetesimal colliding with the Earth, but the general case of a collisionless encounter is similar. The orbit of the Earth and Moon around their common centre of mass is defined by their relative position and velocity. A third body encountering the Earth–Moon binary must have an orbit that crosses the system's heliocentric orbit, and approaches it with some finite velocity at large separation. Hence, the delivery of mass onto the Earth is accompanied by the delivery of external momentum that—in the impulse approximation—changes the relative velocity, but not the relative position, of the Earth with respect to the Moon, altering the mutual orbit, a hitherto overlooked effect that can excite the lunar inclination and eccentricity.

We ask whether the satellite excitation is dominated by the few strongest encounters or by the much more numerous distant ones. Theory suggests that for top-heavy perturber populations, the few strongest perturbations dominate over the more numerous weak ones[28]. We test this theory for our simulations by generating realizations where the impact parameter is chosen in the interval $[0, R_H]$, $[0, R_H/2]$ and $[0, R_H/4]$, progressively eliminating a large number of distant encounters. The results of the three simulations are statistically indistinguishable (see Extended Data Fig. 2a), confirming the theoretical expectation. To facilitate the reproducibility of our results, we plot a measure of the strength of a perturbation against the impact parameter of the encounters for two individual simulations (Extended Data Fig. 2b, c).

The simulations are permitted to proceed until the population of Earth-crossing bodies are exhausted either through collision with the Earth or through loss via another channel in accordance with an average rate (see above). At the end of the simulations, which characteristically last about 10^8 years, the lunar orbit is typically at about $40R_E$. To compare the simulation outcomes to the modern system, we propagate the lunar orbit forward to its current separation at $60R_E$ and permit the inclination to decay in accordance with the action of planetary tides (equation (1)). The number of simulations was chosen such that the median inclination values vary by only several per cent.

Recently, it has been suggested that the lunar inclination could have been damped via obliquity tides in the lunar magma ocean (LMO) as the Moon's obliquity increased during its approach to the Cassini state transition between $20R_E$ and $30R_E$ (ref. 19). The authors of ref. 19 put forward one interpretation of the current excited state of the lunar inclination: that the inclination was excited early[12,13], but that the rate of tidal dissipation in the post-giant-impact Earth was sufficiently low to delay passage of the lunar orbit through the Cassini state transition until after the crystallization of the LMO, at which point the effect of obliquity tides on the lunar inclination becomes much less. With the 'late' mechanism of lunar orbital excitation described here, we identify a different solution: that the rate of tidal dissipation on the post-impact Earth is sufficiently rapid in the first tens of millions of years to carry the Moon through the Cassini state transition and to damp any early acquired lunar inclination. Following such a resetting episode, the LMO crystallizes, and inclination excitation due to encounters is subsequently preserved. To explore this solution, we ran a suite of simulations in which the inclination is reset to zero until a certain time, and permitted to accumulate excitation subsequently (see Extended Data Fig. 3). Such a transition marks the time of crystallization of the LMO. It can be seen

that as long the duration of the LMO crystallization is sufficiently short, such a solution is viable and, indeed, necessary in a tidal evolution scenario recently described[29].

Code availability. The code used to conduct these simulations is available by request from the authors.

23. Walsh, K. J., Morbidelli, A., Raymond, S. N., O'Brien, D. P. & Mandell, A. M. A low mass for Mars from Jupiter's early gas-driven migration. *Nature* **475,** 206–209 (2011).
24. Wetherill, G. W. Collisions in the asteroid belt. *J. Geophys. Res.* **72,** 2429–2444 (1967).
25. Yoder, C. F. & Peale, S. J. The tides of Io. *Icarus* **47,** 1–35 (1981).
26. Kaula, W. M. Tidal dissipation by solid friction and the resulting orbital evolution. *Rev. Geophys.* **2,** 661–685 (1964).
27. Wieczorek, M. A., Weiss, B. P. & Stewart, S. T. An impactor origin for lunar magnetic anomalies. *Science* **335,** 1212–1215 (2012).
28. Collins, B. F. & Sari, R. Levy flights of binary orbits due to impulsive encounters. *Astron. J.* **136,** 2552–2562 (2008).
29. Zahnle, K. J., Lupu, R., Dobrovolskis, A. & Sleep, N. H. The tethered Moon. *Earth Planet. Sci. Lett.* **427,** 74–82 (2015).
30. Marchi, S., Bottke, W. F., Kring, D. A. & Morbidelli, A. The onset of the lunar cataclysm as recorded in its ancient crater populations. *Earth Planet. Sci. Lett.* **325–326,** 27–38 (2012).

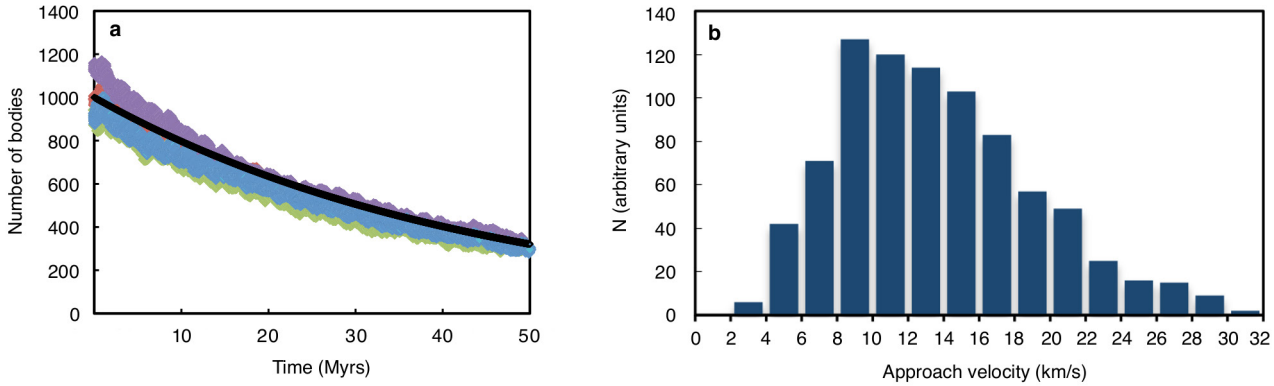

Extended Data Figure 1 | Properties of planetesimal populations. **a**, Decay rates of Earth-crossing planetesimal populations according to *N*-body simulations of the inner Solar System with a resonant (3:2) Jupiter and Saturn at 5.4 AU and 7.2 AU, respectively. Different colours represent the number of Earth-crossing bodies (hence the evolution is not monotonic) in different simulations, from recent integrations[17]. The black line is the prescribed decay rate used in the three-body simulations ($\tau_{SS} = 44$ Myr) to match the decay rate in heliocentric simulations. **b**, Histogram of implemented approach velocities (before acceleration due to Earth gravity) for late-accreting populations in three-body simulations. The population is generated using a Rayleigh distribution of eccentricities and inclinations ($e_R = 0.3$, $i_R = e_R/2$) and a semi-major axis range ($a = 0.8$–1.4 AU) that produces Earth-crossing orbits. These parameters are motivated by simulations of terrestrial planet formation, but the peak of the distribution (9 km s^{-1}) corresponds to the typical encounter velocity inferred for lunar basin-forming impactors[30].

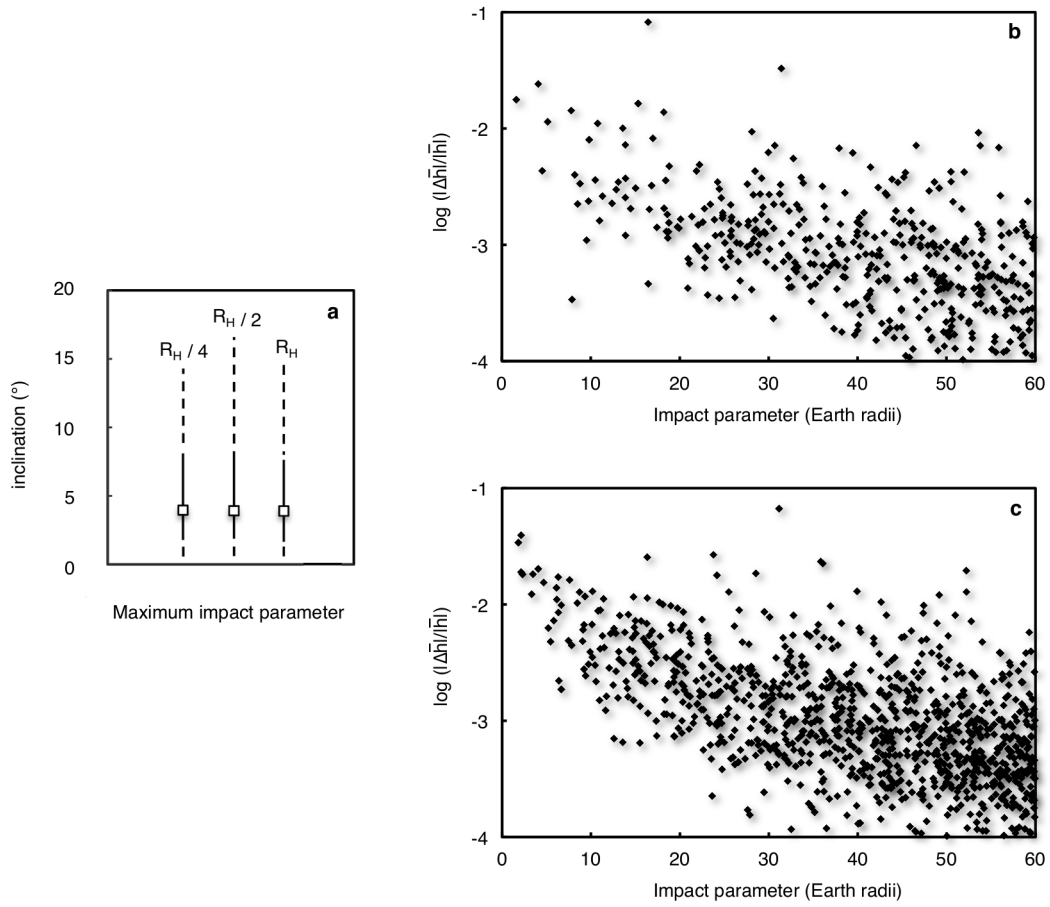

Extended Data Figure 2 | Tests and outcomes for reproducibility. a, Test of the cumulative effect of repeated encounters: median values (squares), and 1σ (solid lines) and 2σ (dashed lines) intervals for three suites of simulations with $0.0075M_E$ accreted via a single body onto an Earth with strong dissipation ($k_2/Q = 0.1$). Each suite of simulations consists of incoming planetesimals with impact parameters (b) ranging from 0 to R_H, $R_H/2$ and $R_H/4$ (as indicated by the values given above each simulation result). The statistical similarity of the resultant distributions shows that distant encounters have a far smaller effect on inclination excitation than do the rare and strong close encounters. **b**, **c**, Distribution of 'kicks' versus impact parameter (b) of encounters from two different realizations. The change in the angular momentum vector of the satellite ($\Delta\bar{h}$) owing to encounter torques is normalized to the magnitude of the orbital angular momentum before the encounter ($\bar{h}$). The planetesimals approaching the Earth–Moon system in this simulation have a mass of $0.0075M_E$. Approach velocities are selected from the distribution plotted in Extended Data Fig. 1b. The cumulative effects of encounters with $b > 60R_E$ are negligible and therefore neglected. Panel **b** (**c**) shows data from a realization that lasts 26.2 Myr (45.3 Myr) and results in a satellite with a final inclination of $i = 1.9°$ ($i = 8.8°$). The strength of tidal dissipation used here ($k_2/Q = 0.1$) quickly results in a satellite semi-major axis of $a = 30R_E$–$40R_E$.

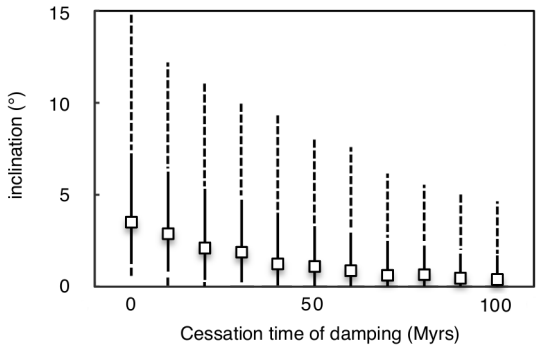

Extended Data Figure 3 | Effect of partial damping due to LMO obliquity tides. Median values (squares), and 1σ (solid lines) and 2σ (dashed lines) intervals for several suites of partially damped simulations. These simulations consist of an accreted mass of $0.0075M_E$ delivered via a single body onto a strongly dissipative ($k_2/Q = 0.1$) Earth, with the orbital excitation continuously reset ($e = 0$, $i = 0$) until a certain time and permitted to accumulate subsequently. Such a transition represents LMO crystallization and the cessation of inclination damping via obliquity tides[19]. These simulations are representative of excitation behaviour for partially damped cases. It can be seen that, so long as the crystallization of the LMO is sufficiently rapid (about 10^7 years), excitation via planetesimal encounters is largely unaffected.